Random-field-induced disordering mechanism in a disordered ferromagnet: Between the Imry-Ma and the standard disordering mechanism

Juan Carlos Andresen,[1,2] Helmut G. Katzgraber,[3,4,5] and Moshe Schechter[2]

[1]*Department of Theoretical Physics, KTH Stockholm, 10691 Stockholm, Sweden*

[2]*Department of Physics, Ben Gurion University of the Negev, Beer Sheva 84105, Israel*

[3]*Department of Physics and Astronomy, Texas A&M University, College Station, Texas 77843-4242, USA*

[4]*1QB Information Technologies (1QBit), 458-550 Burrard Street, Vancouver, British Columbia, Canada V6C 2B5*

[5]*Santa Fe Institute, 1399 Hyde Park Road, Santa Fe, New Mexico 87501, USA*

Random fields disorder Ising ferromagnets by aligning single spins in the direction of the random field in three space dimensions, or by flipping large ferromagnetic domains at dimensions two and below. While the former requires random fields of typical magnitude similar to the interaction strength, the latter Imry-Ma mechanism only requires infinitesimal random fields. Recently, it has been shown that for dilute anisotropic dipolar systems a third mechanism exists, where the ferromagnetic phase is disordered by finite-size glassy domains at a random field of finite magnitude that is considerably smaller than the typical interaction strength. Using large-scale Monte Carlo simulations and zero-temperature numerical approaches, we show that this mechanism applies to disordered ferromagnets with competing short-range ferromagnetic and antiferromagnetic interactions, suggesting its generality in ferromagnetic systems with competing interactions and an underlying spin-glass phase. A finite-size-scaling analysis of the magnetization distribution suggests that the transition might be first order.

I. INTRODUCTION

Spin glasses, where frustration and disorder are introduced through random competing ferromagnetic and antiferromagnetic interactions [1], and random-field ferromagnets, where disorder is introduced through an effective longitudinal field [2], are two archetypal models for the study of disordered magnetic systems [3,4]. While usually studied independently from each other, random interactions and random fields are generic in many nonmagnetic systems [5], and dominate thermodynamic and dynamic properties in, e.g., orientational glasses [6] and relaxor ferroelectrics [7,8]. In magnetic systems, random interactions are abundant, yet the presence of an effective longitudinal random field is nontrivial. Applied magnetic fields cannot be locally randomized and nonmagnetic disorder cannot produce an effective random magnetic field, because it violates time-reversal symmetry.

Anisotropic dipolar magnets, and specifically the $\mathrm{LiHo}_x\mathrm{Y}_{1-x}\mathrm{F}_4$ compound, are an intriguing exception. The interplay of an applied field in the direction transverse to the easy axis of the magnetic holmium ions and the off-diagonal elements of the dipolar interaction gives rise to an effective longitudinal field [9–11]. This field is locally random, transforming spatial disorder coming from the dilution of the Ho ions by the nonmagnetic yttrium ions into a disorder in the effective longitudinal field. Furthermore, as a function of holmium concentration, $\mathrm{LiHo}_x\mathrm{Y}_{1-x}\mathrm{F}_4$ has both a ferromagnetic phase at $x \gtrsim 0.3$ and a spin-glass phase at $0 < x \lesssim 0.3$ including the extreme dilute limit [12–14]. The $\mathrm{LiHo}_x\mathrm{Y}_{1-x}\mathrm{F}_4$ system is therefore ideal for the study of the interplay of competing interactions and effective longitudinal random fields, and the effect of this interplay on the thermodynamic and dynamical properties of the system.

Recently, we have shown [13] that disordered anisotropic dipolar magnets in their ferromagnetic phase are driven into a quasi-spin-glass phase upon the introduction of a *finite* effective random magnetic field which is *considerably smaller than the typical nearest-neighbor interaction*. This occurs also in three space dimensions, where it displays a novel disordering mechanism, intermediate between the standard disordering of a ferromagnet and the Imry-Ma [2] mechanism at dimensions two and below. The disordering field is neither infinitesimal, nor of the order of the interaction. The smallness of the random field at the transition is dictated by the proximity of the system to the zero-field transition between the ferromagnet and the spin-glass phase. Moreover, the disordered phase near the transition consists of neither single spins pointing in the direction of the random field, nor of large ferromagnetic domains, but of finite-size glassy domains, reminiscent of the competing spin-glass phase. We denote this phase "quasi-spin-glass" (QSG) in the regime of low temperatures, where it is frozen, and "paramagnetic QSG" (pQSG) in the high temperature regime. The size of the glassy domains is a function of the magnitude of the disordering field and temperature [9,13,15].

Here we consider a more general model of an Ising magnet where the interactions are short ranged, taken from a Gaussian distribution with a mean ferromagnetic value J_0 and a standard deviation J, and with longitudinal random fields taken from a Gaussian distribution of mean zero and standard deviation H_r. Using jaded extremal optimization [16] and large-scale parallel tempering Monte Carlo simulations [17] we analyze the thermodynamic properties of the system at zero and finite temperature. For zero random field we establish the phase diagram of the system, consisting of low-temperature ferromagnetic (FM) and spin-glass (SG) phases and a high-temperature paramagnetic (PM) phase. The zero-temperature transition between the FM and SG phases occurs at a ratio of $J/J_0 \approx 1.65$. We then analyze the disordering of the FM phase at $J/J_0 < 1.65$ with increasing temperature and

random field. For zero temperature we find that the disordering of the FM phase occurs at finite random field, which is much smaller than the typical interaction, $0 < H_r \ll J_0$, the value of H_r depending on the proximity of the system at zero field to the SG phase. At finite temperature we find that the critical temperature of the FM-to-pQSG transition increases linearly as a function of decreasing random field, down to a rather small value of H_r. Our results here are in agreement with our previous results for the dipolar-interacting LiHo$_x$Y$_{1-x}$F$_4$ system [13], as well as with experimental data for this material [18]. This suggests that the disordering mechanism by finite-size glassy domains is a *generic* feature of disordered ferromagnets with competing interactions in the presence of random fields. By analyzing the distribution of magnetization values near the random-field-driven transition, we find evidence for a first-order transition between the FM and pQSG phases in the regime where the FM phase is in proximity to the SG phase. No evidence for a first-order transition is found in the regime where the interactions are strongly ferromagnetic dominated, i.e., $J/J_0 \ll 1$.

The paper is structured as follows. In Sec. II we introduce the model. In Sec. III we introduce the methods used for zero-temperature and for finite-temperature calculations. Our results are presented in Sec. IV, and discussion and conclusions are given in Sec. V. An Appendix lists all parameters of the different simulations.

II. MODEL

The model we simulate is given by the Hamiltonian

$$\mathcal{H} = -\sum_{\langle i,j \rangle} J_{ij} S_i S_j - \sum_i h_i S_i, \qquad (1)$$

where the sum is over nearest neighbors, the spin couplings J_{ij} are chosen from a Gaussian distribution with standard deviation J and mean J_0, and the S_i are Ising spins on the vertices of a hypercube of dimension $d = 3$ and linear size L. Throughout this work we fix the mean of the distribution $J_0 = 1$ and use the standard deviation of the Gaussian distribution J as a means of tuning the interaction disorder in the model. The second term describes the coupling of the Ising spins to a site-dependent random field h_i. The random fields are taken from a Gaussian distribution with zero mean and standard deviation H_r.

Different parameters of the model lead to different phase diagrams. If J is small compared to $|J_0|$ and $H_r = 0$, as the temperature is reduced, the system undergoes a phase transition from a PM phase to a FM phase for $J_0 > 0$. For $J_0 < 0$ the system undergoes a phase transition from a PM phase to an antiferromagnetic (AFM) phase. By increasing the value of the parameter J it is possible to introduce disorder and frustration into the system. These two ingredients are known to be essential for the emergence of a SG phase. The ratio J_0/J quantifies the amount of interaction disorder in the system. Below a critical ratio J_0/J_c, the system has a PM phase at high temperatures and a SG phase at low temperatures (keeping $H_r = 0$). Extreme cases occur when $J = 0$, $J_0 \neq 0$ ($J_0/J \to \infty$) where the model reduces to the well-known Ising model if $H_r = 0$, and to the random-field Ising model [2] if $H_r > 0$; and when $J \neq 0$, $J_0 = 0$ ($J_0/J = 0$)
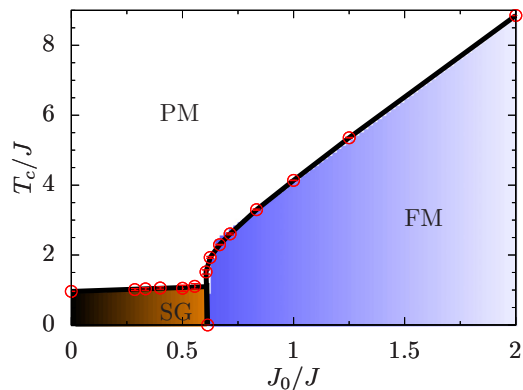

FIG. 1. Dimensionless temperature T/J vs mean of the disorder distribution J_0/J phase diagram for the model given in Eq. (1) with fixed $J_0 = 1$ and $H_r = 0$. At $J \lesssim 1.65$ ($J_0/J \gtrsim 0.606$) and low temperatures the system is in a FM phase. For $J \gtrsim 1.65$ ($J_0/J \lesssim 0.606$) and low temperatures the system is in a SG phase. At high temperatures the system is in the PM phase independently of the value of J_0/J. Note that the model reduces to the three-dimensional Ising model for $J = 0$ and to the EA spin glass for $J_0 = 0$.

where the model reduces to the Edwards-Anderson (EA) spin-glass model [1]. In Fig. 1 we plot the phase diagram of the system as a function of temperature and interaction disorder J (keeping $H_r = 0$) presenting a phase transition at zero temperature between a FM phase at small disorder and a SG phase at large disorder, as well as a PM phase at high temperatures.

The random-field term in Eq. (1) introduces a third axis to Fig. 1. For both limits of zero J and finite J_0 (pure ferromagnet) and zero J_0 and finite J (pure EA spin glass) the effect of finite random field has been thoroughly studied [4,19–29]. For the latter limit two different pictures to describe finite-dimensional spin glasses have been proposed: the replica symmetry breaking (RSB) picture based on the solution of the Sherrington-Kirkpatrick model [30–34], which predicts the existence of a spin-glass phase at finite fields, and the droplet picture [27,28,35,36], which contrary to the RSB predicts the instability of the spin-glass phase for any infinitesimal small field. Which of these pictures correctly describes the three-dimensional spin glass is still an open question [29,37–43]. In this paper, our theoretical considerations are based on the droplet picture, but we do not undermine the possibility to derive an analogous prediction within the RSB picture. Specifically, within the droplet picture of spin glasses, it is argued [27] that the spin-glass phase is unstable to infinitesimal random fields, as finite-size glassy domains are created, destroying long-range glass order. Here we study the effect of the random field in the range, where the system is a ferromagnet, albeit with competing interactions ($0 < J/J_0 < 1.65$). At $T = 0$ we obtain the phase diagram as a function of J and H_r. At finite temperature we obtain the phase diagram for different values of J in the ferromagnetic regime, in proximity to the spin-glass phase and deep inside the ferromagnetic regime. We find the dependence of the critical temperature T_c on random-field strength and study the nature of the phase transition.

III. METHODS

A. Zero-temperature simulations

For the zero-temperature simulations we use the jaded extremal optimization heuristic [16,44]. We set the algorithm parameter $\tau = 1.6$, 1.8, 1.9 with an aging parameter $\Gamma = 0.0001$ for at least 2^{24} simulation steps. Each disorder realization undergoes at least 512 independent runs. We monitor how many times the lowest energy configuration is found. When the success rate is more than $\sim 5\%$, we assume to have found the ground-state configuration. Ground states are found with high confidence for $L \leqslant 10$ for $H_r = 0$ and $L \leqslant 8$ for $H_r \neq 0$.

The FM to SG (PM) phase boundary is identified through the Binder ratio [45]

$$g = \frac{1}{2}\left(3 - \frac{[m^4]_{\mathrm{av}}}{[m^2]_{\mathrm{av}}^2}\right), \tag{2}$$

where $m = 1/N \sum_i S_i$ is the magnetization of the system, $N = L^3$ is the number of spins, and $[\cdots]_{\mathrm{av}}$ represents a disorder average. The Binder ratio g is a dimensionless observable that scales as $g \sim \tilde{G}[L^{1/\nu}(J - J_c)]$. The argument vanishes if $J = J_c$ for all linear system sizes L. Therefore, the crossing of the curves for different system sizes gives an estimate of the transition value J_c up to finite-size effects. Simulation parameters are shown in Table IV.

The critical disorder J_c and the standard deviation for each random field H_r are estimated using a Levenberg-Marquardt minimization combined with a bootstrap analysis, where we assume that the universal function g is well approximated by a third-order polynomial. We show in Fig. 2 how the estimated J_c agrees with the crossing of the Binder ratio curves when $H = 0.00$. The dashed lines are fit functions to the data used only for visualization purposes and the vertical line is the average of the intersections of all samples, in this case $J_c = 1.63(1)$.
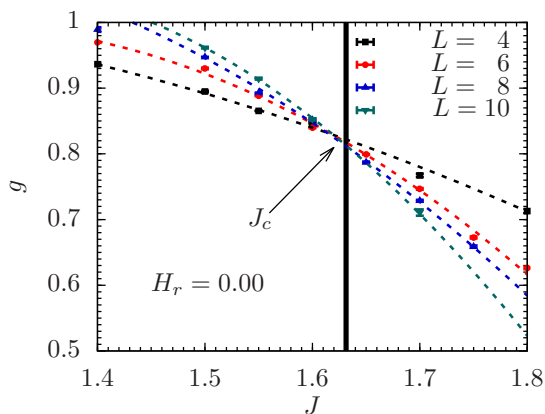

FIG. 2. Binder ratio g as given by Eq. (2) for linear system sizes $L = 4$, 6, 8, and 10 at a random field strength $H_r = 0$ and $T = 0$. The crossing of the curves for different sizes L gives an estimate of the critical disorder J_c denoting the transition between the FM phase at $J < J_c$ and the SG phase at $J > J_c$. The dashed lines are guides to the eye.

B. Finite-temperature simulations

The simulations at finite temperature are done using a combination of single-spin-flip Monte Carlo with parallel tempering Monte Carlo [17]. To determine the finite-temperature transitions for a fixed random field strength H_r and disorder J we measure the ferromagnetic and spin-glass two-point correlation length [46]

$$\xi_L^{\mathrm{sg,fm}} = \frac{1}{2 \sin(k_{\min}/2)}\sqrt{\frac{\chi_{\mathrm{sg,fm}}(\mathbf{0})}{\chi_{\mathrm{sg,fm}}(\mathbf{k}_{\min})} - 1}, \tag{3}$$

where $\mathbf{k}_{\min} = (2\pi/L,0,0)$, $\chi_{\mathrm{sg}}(\mathbf{k})$ is the spin-glass wave-dependent susceptibility

$$\chi_{\mathrm{sg}}(\mathbf{k}) = \frac{1}{N}\left[\left\langle \sum_{i,j} q_i q_j e^{i\mathbf{k}\mathbf{r}_{ij}} \right\rangle\right]_{\mathrm{av}}, \tag{4}$$

$q_i = S_i^\alpha S_i^\beta$ is the two-replica spin overlap, and $\chi_{\mathrm{fm}}(\mathbf{k})$ is the ferromagnetic wave-dependent susceptibility

$$\chi_{\mathrm{fm}}(\mathbf{k}) = \frac{1}{N}\left[\left\langle \sum_{i,j} S_i S_j e^{i\mathbf{k}\mathbf{r}_{ij}} \right\rangle\right]_{\mathrm{av}}. \tag{5}$$

Here $\langle \cdots \rangle$ denotes a thermal average and $[\cdots]_{\mathrm{av}}$ a disordered average.

Near the transition the dimensionless ratio of the two-point correlation functions $\xi_L^{\mathrm{sg,fm}}$ and the linear system size L scales as $\xi_L^{\mathrm{sg,fm}}/L \sim \tilde{X}[L^{1/\nu}(T - T_c)]$. At the critical temperature the argument vanishes and the dimensionless quantity becomes size independent (up to scaling corrections), hence we expect lines of different system sizes to cross at T_c. If, however, the lines do not cross, no transition takes place at the studied temperature range. Some example cases are shown in Fig. 3. In Fig. 3(a) the FM two-point correlation length for $J = 1.60$ ($J_0/J = 0.625$) and $H_r = 0.00$ is depicted. Clearly the curves cross at a putative point which indicates a transition at a temperature T_c. In Fig. 3(b) we plot the same quantity, but for a higher disorder value $J = 1.80$ ($J_0/J = 0.5\bar{5}$). In this case, clearly the curves do not intersect at any studied temperature, showing a lack of a ferromagnetic phase transition in this temperature range. Moreover, it suggests a possible lack of ferromagnetic transition at any $T > 0$. In Fig. 3(c) we show the spin-glass two-point correlation length for the same disorder value $J = 1.80$ as in Fig. 3(b). The curves do cross in the simulated temperature range, signaling a PM to SG phase transition.

For small random field strengths and interactions distribution widths the equilibration time is relatively short, making it possible to simulate large system sizes. With increasing random fields and interaction distribution widths equilibration times become longer. To determine the critical temperature we approximate the scaling function by a third-order polynomial and perform a fit with six free parameters. To estimate the error bars we use a bootstrap analysis as described by Katzgraber *et al.* [47]. Simulation parameters for the finite-temperature simulations are shown in Tables I, II, and III.
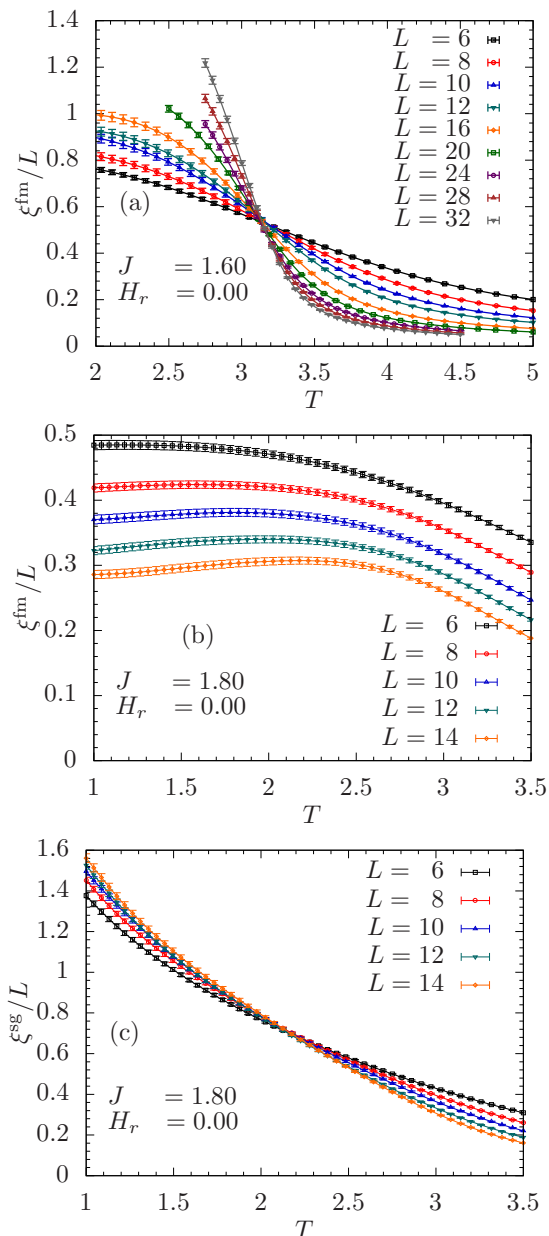
FIG. 4. J-H_r phase diagram at $T = 0$. At $H_r = 0$ there is a FM-SG transition at $J_c(0) = 1.63$. At finite but small H_r the disordered paramagnetic phase has finite size glassy domains, denoted here as a "quasi-SG" (QSG) phase. The crossover between the QSG phase and the PM phase with short range spin-spin correlations is speculative. In the inset, the solid black line is a fit $H_r(J^{-1}) = \alpha (J^{-1} - J_c^{-1})^\beta$ to the data at low random field strength. Here J_c and β are fixed parameters; we use the above estimated value $J_c(0) = 1.63$, and the analytical result of Ref. [13] $\beta = 0.466$. $\alpha = 1.52(17)$ is a free fitting parameter.

FIG. 3. Ferromagnetic and spin-glass two-point correlation functions divided by the linear system size L for $J = 1.60$ (a) and 1.80 (b) and (c), respectively. (a) The crossing of the curves of the dimensionless quantity ξ_L^{fm}/L for linear system sizes $L = 6$–20 indicates that a PM to FM transition occurs at $T_c \sim 3.09(4)$. (b) The dimensionless quantity ξ_L^{fm}/L does not cross in the studied temperature range, showing the lack of a FM transition. (c) Curves corresponding to different system sizes of the dimensionless quantity ξ_L^{sg}/L cross at $T_c \sim 1.90(14)$ indicating that a PM to SG transition occurs in this temperature range.

IV. RESULTS

The phase diagram of the model presented in Sec. II is shown in Fig. 1. It has a high temperature PM phase and low temperature FM and SG phases at small and strong disorder J, respectively. The boundary between the FM and the SG phase is at $J \approx 1.65$ ($J_0/J \approx 0.606$) with a weak reentrance at $T = 0$ [$J_c = 1.63(1)$]. The obtained phase diagram qualitatively
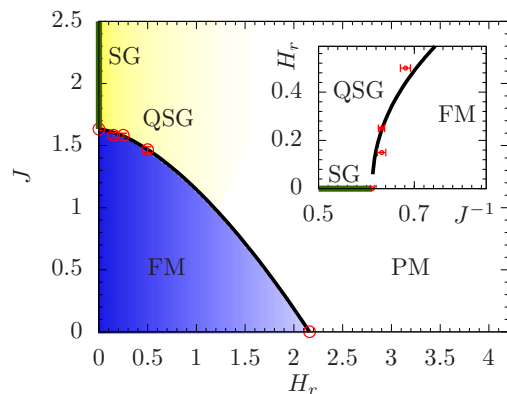
agrees with previous results [48–50] for the model in Eq. (1), and for the closely related diluted bimodal Ising SG model [51]. In comparison to the real space rescaling method by Southern and Young [50], we find larger values for T_c and for J_c, in accordance with the typical behavior of real-space rescaling method [50]. Note the linear dependence of the PM to SG transition on the mean interaction value. The same is true for the PM to FM phase transition in the regime $J \lesssim 1.2$ ($J_0/J \gtrsim 0.83\bar{3}$).

We now study the phase diagram with the inclusion of finite random fields and consider first the case where $T = 0$, see Fig. 4. The FM phase at low disorder J and low random-field strength H_r is disordered at large J into a QSG phase, consisting of finite size glassy domains, but no long range glass order except at $H_r = 0$. The data point at $H_r = 0$ corresponds to the FM to SG transition point at $T = 0$ plotted also in the T/J vs J_0/J phase diagram shown in Fig. 1. At small J and large H_r the FM phase disorders into a PM phase. The data point at $J = 0$ corresponds to the critical random field value $H_r \approx 2.16$ of the random-field Ising model. For low disorder J we expect the critical random field to be of the order of the mean interaction J_0, because in the PM phase single spins order along their local effective field.

The situation for $J \lesssim J_c$ is, however, different. At $H_r = 0$ the FM ground state and the lowest-energy SG state differ in energy, the difference being linear in $J - J_c$ [13]. At finite H_r, the low-energy SG state changes profoundly: long-range order is destroyed, finite-size glassy domains appear, and the energy of the resulting QSG state is reduced accordingly [9,13]. This leads to a reduction of the energy of the QSG state below that of the ferromagnetic state, and thus to a zero-temperature phase transition at finite H_r, which is much smaller than J_0. The predicted functional form for the boundary between the
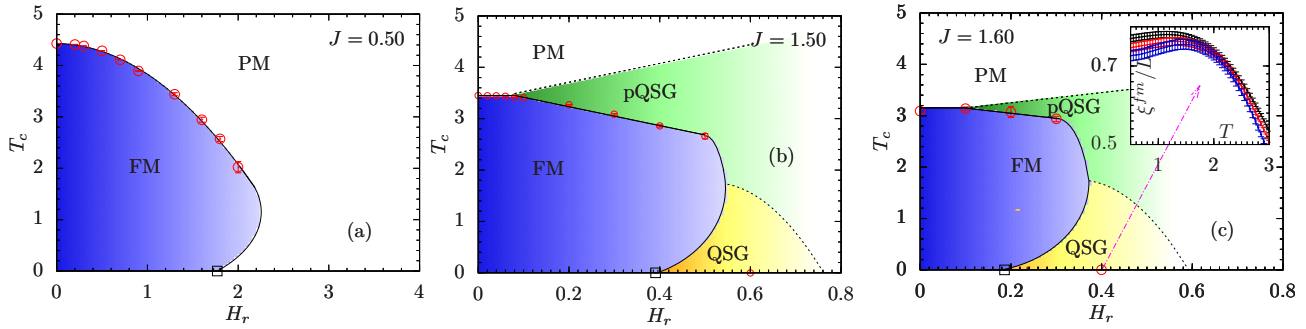
FIG. 5. T-H_r phase diagram for $J = 0.50$ (a), $J = 1.50$ (b), and $J = 1.60$ (c). For the slightly disordered system with $J = 0.50$ in (a) the relation expected from mean-field theory $T(H_r) - T_c \sim H_r^2$ holds, except for a weak reentrance at the lowest temperatures. The data are consistent with the disordered phase being a standard PM. For the highly disordered systems with $J = 1.50$ (b) and $J = 1.60$ (c) where the FM phase is close to the SG phase at $H_r = 0$ (see Fig. 4) we find a linear relation $T(H_r) - T_c(h^*) \propto H_r$ for $H_r > h^*$ consistent with the disordered phase being a pQSG. Furthermore, we find strong reentrance at low temperatures with critical $H_r \ll J_0$, in agreement with the disordered phase being a QSG. The inset in (c) shows ξ_L^{fm} for $L = 8$, 10, and 12 for $H_r = 0.40$ where the curves do not cross, indicating the lack of a phase transition to the FM phase for the studied temperature range. The dashed lines in all panels between the pQSG and PM phases and between the QSG and pQSG phases denote smooth crossovers, their functional form should be considered as a guide to the eye.

FM and the PM phases at $T = 0$ is given by [13]

$$H_r(J^{-1}) \propto \left(J^{-1} - J_c^{-1} \right)^{\frac{(3/2-\theta)}{(3-\theta)}}. \quad (6)$$

Here $\theta \approx 0.19$ is the stiffness exponent [52]. Indeed, our numerical results are in agreement with this functional form, as can be seen by fitting the data for $H_r < 1$, fixing the power to its theoretically obtained value [13] $\beta = (3/2 - \theta)/(3 - \theta) = 0.466$, and using the above estimated critical disorder $J_c \approx 1.63$ for the fit. This leaves the proportionality prefactor α as the single free fitting parameter. The inset of Fig. 4 shows the fitting result. We note that our data are limited to $H_r \leqslant 0.5$. It was not possible to determine the crossing point of the Binder ratio curves for different system sizes for random fields with $H_r > 0.5$ because of the proximity of the crossing point to $g = 1$.

At finite temperature and for $J \lesssim J_c$, similar considerations to the ones mentioned above manifest themselves in the dependence of T_c on the random field. The underlying glassy state at finite temperature consists of paramagnetic SG domains of typical size ξ. We denote this phase as pQSG. For moderate H_r, which does not affect the typical domain size, the reduction of the energy per spin of the pQSG state is $\propto H_r/\xi^{3/2}$. As a result, only for $H_r > h^* \propto (J_c - J)\xi^{3/2}$ the disordering of the FM phase is by the pQSG phase. In this regime theory predicts a linear dependence of T_c on H_r [13]. At $H_r < h^*$ the disordering is to the standard PM phase, with the known weak dependence of T_c on H_r. All the above considerations do not apply to $J \ll J_c$, where the FM is far from the SG phase, and the disordering to the PM phase is standard for all strengths of random field.

In Fig. 5 we present the T vs H_r phase diagrams for disorders $J = 0.50$, $J = 1.50$, and $J = 1.60$. In Fig. 5(a) $J \ll J_c$. The disordering is into the standard PM phase, with quadratic dependence $T(H_r) - T_c(0) \propto H_r^2$ for small H_r and a small reentrance at low temperatures. For $J = 1.50$ [Fig. 5(b)] the system is close to the SG phase. Indeed, for $H_r < h^* \approx 0.1$ the dependence of T_c on H_r is weak, as is expected for disordering to the standard PM phase. For $H_r > h^*$ we find

the dependence of T_c on H_r to be linear, in agreement with disordering to the pQSG phase. We note that at $0.5 < H_r < 0.6$ there is a sharp decrease of T_c to zero within the finite-temperature simulations, and we find a value of $H_r = 0.39$ for the zero temperature transition (inferred from the fitting function in the inset of Fig. 4). This is in agreement with the disordering field by the QSG phase being much smaller than the interaction strength also at low temperatures. We note that as the QSG phase is frozen, susceptibility measurements are expected to depict only the crossover between the QSG and the PM phase at large random fields. This is in agreement with Ref. [18], where a sharp feature in the susceptibility is observed at higher temperatures, depicting the transition to the pQSG phase, but a smooth crossover is observed for the lower temperatures. The observed peak value at the crossover occurs at larger H_r with diminishing peak value as temperature is reduced [18], in agreement with the scenario of the QSG having smaller glassy domains as a function of increasing H_r [9,13]. In Fig. 5(c) we present the results for $J = 1.60$, closer to the zero-field FM-to-SG transition. Results are similar to the case of $J = 1.50$, with a weaker linear dependence, and with a smaller random field $0.3 < H_r < 0.4$, which disorders the FM at all temperatures.

Let us now consider the order of the FM to PM/pQSG transition. The order of the phase transition of the RFIM is a long standing question. Whereas analytic arguments support a second-order transition controlled by a zero-temperature fixed point [27,53,54], some numerical results support a first-order transition [19,20] while others support a second-order transition [21,22,55–59]. For bimodal disorder distributions a mean-field solution suggests a first-order transition for large enough values of the random field [60]. Recent numerical work supports universality in the RFIM [58], suggesting that the nature of the phase transition is independent of the random-field distribution. Moreover, high-accuracy estimates for the magnetic exponent ratio β/ν [59] found the value to be very small, but clearly finite. In the present work, for small exchange disorder ($J = 0.50$) we do not find any signature of a first-order phase transition. This suggests that the recent phase
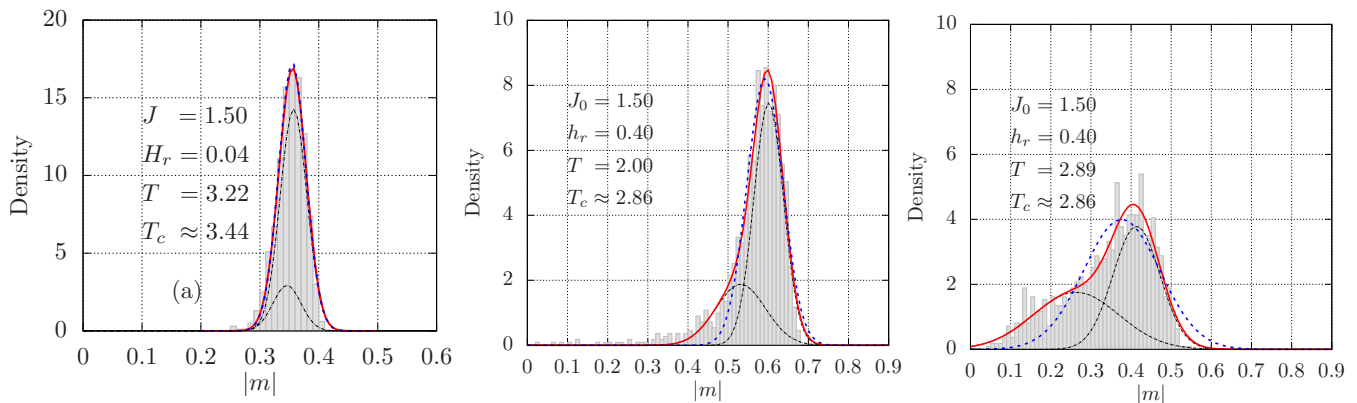
FIG. 6. Magnetization histograms for $J = 1.50$ with a random field $H_r = 0.04$ and $L = 40$ (below the critical temperature) (a), $H_r = 0.40$ and $L = 20$ (below the critical temperature) (b), and $H_r = 0.40$ and $L = 20$ (above the critical temperature) (c). The solid red lines are double-Gaussian fits, which are composed of the sum of the two modes (thin dashed black lines), the blue dashed lines are single Gaussian fits. For $H_r = 0.04$, the double Gaussian fit does not differ much from the single Gaussian fit, i.e., the distribution is normally distributed as expected for all temperatures in a continuous phase transition. For $H_r = 0.40$ a hump emerges for $T < T_c$, the single Gaussian fit (blue dashed line) cannot capture the hump, but the double Gaussian fit (solid red line) does. Close to the critical temperature the single Gaussian fails to fit the distribution and a bimodal double-Gaussian structure becomes evident suggesting a finite jump in the magnetization washed out by the disorder at T_c, as expected for a first-order phase transition.

transition behavior found for the RFIM [58,59] also applies for models with small exchange disorder.

We now consider the order of the transition in the presence of both random fields and strong random interactions. Intriguingly, our results suggest, for strong interaction disorder, a continuous transition for $H_r < h^*$ where the FM disorders into a "standard" PM phase, and a first-order transition for $H_r > h^*$ where the disordering is into the pQSG phase. In the latter, we find a discontinuous jump in the magnetization across the transition, but from our microcanonical simulations, based on a recently proposed method [61–63], we did not detect any latent heat, which is either zero or too small to be detected in the current accessible system sizes, similar to Refs. [20,21].

Specifically, we study the distribution of the magnetization above and below T_c for $J = 1.50$ at different field strengths H_r, as shown in Fig. 6. A bimodal distribution close to T_c is a sign of a first-order phase transition, whereas a normal distribution with mean $\mu_0 = [\langle |m| \rangle]_{av}$ would be the expected distribution for a continuous phase transition. For small $H_r = 0.04 < h^*$ [Fig. 6(a)] we note that the single-Gaussian fit and the double-Gaussian fit agree, suggesting that the magnetization distribution is likely normal close to T_c and therefore the phase transition is continuous. However, we find that for large $H_r = 0.40 > h^*$ the double-Gaussian fit does differ considerably from the single-Gaussian fit, moreover, the double Gaussian fit reproduces better the magnetization histogram below and above T_c. This suggests that the magnetization
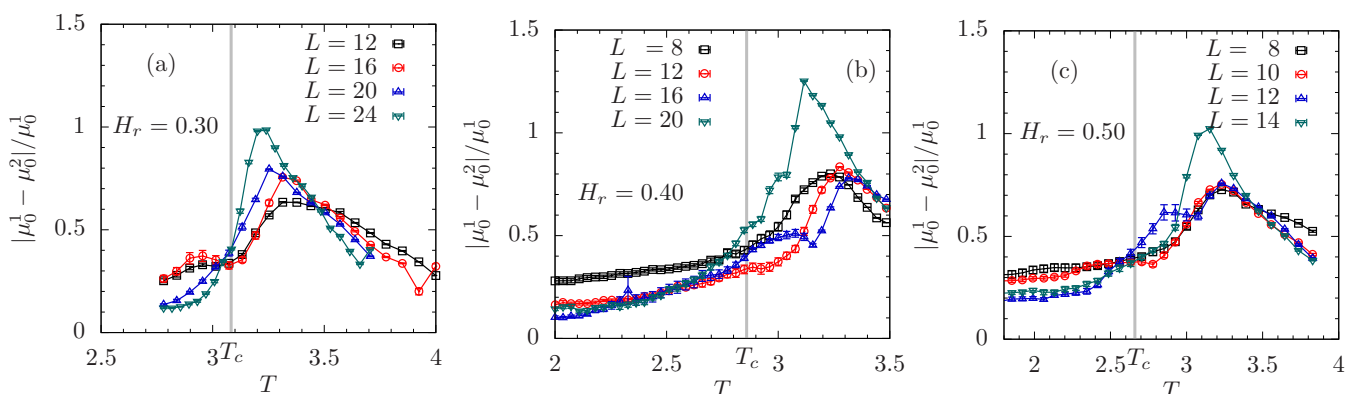
FIG. 7. Relative difference of the bootstrapped mean value of the two modes (with mean values μ_0^1 and μ_0^2) of the bimodal Gaussian fitted function as a function of temperature for (a) $H_r = 0.30$, (b) $H_r = 0.40$, and (c) $H_r = 0.50$. The gray vertical line corresponds to the estimated critical temperature. The relative difference between the modes increases close to T_c, the discrepancy between the estimated value for T_c and the maximal values of the curves can be attributed to the strong finite-size correction of this observable.

jumps at T_c, and thus the existence of a first-order phase transition.

To strengthen the claim of a bimodally distributed magnetization for large random fields close to T_c, we perform a bootstrap analysis of the double-Gaussian fit for $J = 1.50$ and $H_r = 0.30$, 0.40, and 0.50, and show the normalized difference between the mean of the two modes as a function of the temperature T (see Fig. 7). We observe that the maximum values of the curves are close to T_c. The fact that the relative difference between the modes is maximal close to the critical temperature gives further evidence for a first-order phase transition. These distributions show large finite-size corrections and a clean determination of the critical temperature is difficult.

V. DISCUSSION

Disordered nonmagnetic ferroic systems naturally show randomness in both their interparticle interactions and in the effective field presented as a bias between the two degenerate single-particle states. Recently, it was shown that this interplay of randomness of interactions and fields is present also in the ferromagnetic phase of the $LiHo_xY_{1-x}F_4$ compound. This has allowed for new experiments [18,64] investigating this interplay of randomness, as well as for new insights into older experiments, e.g., demonstrating different final states obtained by in-field and zero-field annealing of the disordered ferromagnetic $LiHo_xY_{1-x}F_4$ system [65].

The effective random field in the $LiHo_xY_{1-x}F_4$ system is a consequence of the interplay between the off-diagonal terms of the dipolar interactions and the applied transverse field. The applied field also induces transitions between the spin up $|\uparrow\rangle$ and spin down $|\downarrow\rangle$ states in Ho, thus giving rise to an effective transverse field term in the Ising Hamiltonian. However, at low field, the effective random field dominates because it is linear in the applied transverse field [9,11], whereas the effective transverse field is negligible at small fields [66,67].

In a previous study [13] we analyzed the $LiHo_xY_{1-x}F_4$ system in the regime where the system is ferromagnetic, albeit with disorder in both the interaction and the effective longitudinal field. We have suggested a novel disordering mechanism where at a finite random field that is much smaller than the typical interaction, finite-size glassy domains disorder the FM phase into a PM phase. This mechanism explains various experimental features, such as the linear dependence of the critical temperature with increased random field, and the diminishing and rounding of the susceptibility peak with decreasing temperature [18].

The scaling theory within which the novel disordering mechanism was obtained [13] is not particular to dipolar systems. In the present work we have shown that the same mechanism applies to a *generic* short-range random-field Ising model with competing interactions having a ferromagnetic mean. Our results thus support the generality of the disordering mechanism to random-field ferroic systems with competing interactions, and it would be of interest to check their applicability, e.g., to relaxor ferroelectrics [7,8,68,69].

We find an excellent agreement, quantitative and qualitative, between our numerical results and the predictions of the scaling theory based on the picture of the disordering of a FM with competing interactions by a QSG (pQSG) phase at low (high) temperature. It would be of much interest to further corroborate our results here with a direct microscopic analysis of the domain structure in the disordered phase.

We further analyze here the nature of the FM to PM transition and show evidence suggesting that once the disordering is induced via the above-mentioned mechanism, where the FM phase is disordered by finite size glassy domains (i.e., to the pQSG phase), then the transition is first order. This differs from the RFIM with no competing interaction. In the latter, it is believed that the thermodynamic phase transition is second order [2], albeit experimentally hard to be observed because of slow relaxation. It would be of much interest to further study this transition between the FM and pQSG phases, and the dynamics of the system near the transition, as hysteresis and slow relaxation are expected. With regard to the latter, nonequilibrium dynamics of the Ising model were recently studied in the presence of random bonds [70] or in the presence of random fields [71]. For both systems it was shown that the equilibrium disorder-driven transition shows up when measuring the nonequilibrium aging properties. It would be of interest to study whether the quasi-SG driven transition discussed here has distinct characteristics in the nonequilibrium aging properties of the system.

APPENDIX

The simulation parameters for Fig. 5 are shown in Tables I, II, and III for $\tilde{J} = 0.50$, $\tilde{J} = 1.50$, and $\tilde{J} = 1.60$, respectively. The simulation parameters of the zero-temperature simulations are shown in Table IV.

TABLE I. Parameters of the simulations for $\tilde{J} = J/J_0 = 0.5$, where $J_0 = 1$. N_{sa} is the number of samples, N_{sw} is the total number of Monte Carlo sweeps used for equilibration, T_{min} is the lowest temperature simulated, T_{max} is the highest temperature simulated, and N_T is the number of temperatures used in the parallel tempering method for each system size L.

$\tilde{J}$	H_r	L	N_{sa}	N_{sw}	T_{min}	T_{max}	N_T
0.50	0.00	16,20,24	512	1024	4.200	5.000	100
0.50	0.00	28,32	512	2048	4.200	5.000	100
0.50	0.00	40	512	4096	4.200	5.000	100
0.50	0.00	48	512	8192	4.200	5.000	40
0.50	0.20	16,20,24	512	2048	4.100	5.000	30
0.50	0.20	28,32,36,40	512	2048	4.100	5.000	50
0.50	0.30	16,20,24	1024	2048	4.100	5.000	30
0.50	0.30	28,32	512	2048	4.100	5.000	50
0.50	0.30	40	512	4096	4.100	5.000	50
0.50	0.50	16	1024	4096	4.100	5.000	30
0.50	0.50	20	1024	8192	4.100	5.000	30
0.50	0.50	24	1024	16384	4.100	5.000	30
0.50	0.50	28,32,40	1024	16384	4.100	5.000	50
0.50	0.70	16	1024	2048	3.950	4.850	30
0.50	0.70	20	1024	8196	3.950	4.850	30
0.50	0.70	24	1024	16384	3.950	4.850	30
0.50	0.70	28,32,40	1024	16384	3.950	4.850	50
0.50	0.90	12	1024	1024	3.700	4.800	30
0.50	0.90	16	1024	4096	3.700	4.800	30
0.50	0.90	20	1024	8192	3.700	4.800	30
0.50	0.90	24	1024	16384	3.700	4.800	30
0.50	0.90	28,32	1024	65536	3.700	4.800	40
0.50	1.30	12	1024	512	2.200	5.000	40
0.50	1.30	16	1900	32768	2.200	5.000	50
0.50	1.30	20	1424	262144	2.200	5.000	50
0.50	1.30	24	1424	1048576	2.200	5.000	50
0.50	1.60	8	2300	8192	1.500	5.000	50
0.50	1.60	10	2300	65536	1.500	5.000	50
0.50	1.60	12	2073	4194304	1.500	5.000	50
0.50	1.60	14	2116	4194304	1.500	5.000	50
0.50	1.80	6	1274	32768	1.400	5.000	50
0.50	1.80	8	2230	65536	1.400	5.000	50
0.50	1.80	10	2392	2097152	1.400	5.000	50
0.50	1.80	12	2752	16777216	1.400	5.000	50
0.50	2.00	4,6	3000	16384	0.600	4.500	50
0.50	2.00	8	4500	1048576	0.600	4.500	50
0.50	2.00	10	1200	33554432	0.600	4.500	50

TABLE II. Parameters of the simulations for $\tilde{J} = J/J_0 = 1.50$, where $J_0 = 1$. N_{sa} is the number of samples, N_{sw} is the total number of Monte Carlo sweeps used for equilibration, T_{min} is the lowest temperature simulated, T_{max} is the highest temperature simulated, and N_T is the number of temperatures used in the parallel tempering method for each system size L.

$\tilde{J}$	H_r	L	N_{sa}	N_{sw}	T_{min}	T_{max}	N_T
1.50	0.00	16,20	1024	16384	3.30	3.80	100
1.50	0.00	24,28	1024	65536	3.30	3.80	100
1.50	0.00	32,40	1024	262144	3.30	3.80	30
1.50	0.02	16	1024	65536	3.22	3.983	18
1.50	0.02	20,24	1024	65536	3.22	3.983	30
1.50	0.02	28	1024	131072	3.22	3.983	30
1.50	0.02	32,40	1024	131072	3.22	3.983	40
1.50	0.04	16	1024	65536	3.22	3.983	18
1.50	0.04	20	1024	65536	3.22	3.983	40
1.50	0.04	24,28,32,40	1024	131072	3.22	3.983	40
1.50	0.06	16	1024	32768	3.22	3.983	18
1.50	0.06	20,24	1024	65536	3.22	3.983	40
1.50	0.06	28,32	1024	262144	3.22	3.983	40
1.50	0.06	40	1200	524288	3.22	3.983	40
1.50	0.08	16,20	1024	16384	3.25	4.00	20
1.50	0.08	24	1024	65536	3.22	4.00	18
1.50	0.08	28	1024	262144	3.22	4.00	40
1.50	0.08	32,40	1024	524288	3.22	4.00	40
1.50	0.10	16	2048	16384	3.20	4.00	16
1.50	0.10	20	2048	32768	3.20	4.00	16
1.50	0.10	24	1024	65536	3.20	4.00	16
1.50	0.10	28	1024	262144	3.20	4.00	40
1.50	0.10	32,40	1024	524288	3.20	4.00	40
1.50	0.20	12	2048	16384	3.00	4.00	16
1.50	0.20	16	1024	32768	3.00	4.00	16
1.50	0.20	20,24	1024	131072	3.00	4.00	16
1.50	0.20	28,32	1024	524288	3.00	4.00	30
1.50	0.30	12,14	2048	32768	2.78	4.00	20
1.50	0.30	16	1024	65536	2.78	4.00	20
1.50	0.30	20	2043	131072	2.78	4.00	20
1.50	0.30	24	3285	1048576	2.78	4.00	30
1.50	0.40	8,10,12	2048	32768	2.00	4.50	60
1.50	0.40	14,16	2048	65536	2.00	4.50	60
1.50	0.40	20	1024	1048576	2.00	4.50	60
1.50	0.50	4	4096	32768	1.00	5.00	50
1.50	0.50	6	3637	65536	1.00	5.00	50
1.50	0.50	8	2048	131072	1.00	5.00	50
1.50	0.50	10	2048	262144	1.00	5.00	50
1.50	0.50	12	1441	1048576	1.00	5.00	50
1.50	0.50	14	2645	2097152	1.00	5.00	50
1.50	0.60	4,6	2048	16384	1.00	5.00	50
1.50	0.60	8	1387	65536	1.00	5.00	50
1.50	0.60	10	2048	262144	1.00	5.00	50
1.50	0.60	12	5275	524288	1.00	5.00	50
1.50	0.60	14	1199	4194304	1.00	5.00	50
1.50	0.60	16	1024	33554432	1.00	5.00	50

TABLE III. Parameters of the simulations for $\tilde{J} = J/J_0 = 1.60$, where $J_0 = 1$. N_{sa} is the number of samples, N_{sw} is the total number of Monte Carlo sweeps used for equilibration, T_{min} is the lowest temperature simulated, T_{max} is the highest temperature simulated, and N_T is the number of temperatures used in the parallel tempering method for each system size L.

$\tilde{J}$	H_r	L	N_{sa}	N_{sw}	T_{min}	T_{max}	N_T
1.60	0.00	12	1024	8192	2.75	5.00	100
1.60	0.00	16	1024	32768	2.75	5.00	100
1.60	0.00	20	1024	65536	2.75	5.00	100
1.60	0.00	24	1024	262144	2.75	5.00	30
1.60	0.00	28	1024	524288	2.75	5.00	30
1.60	0.00	32	1024	1048576	2.75	5.00	30
1.60	0.10	12	1024	32768	1.75	5.00	37
1.60	0.10	16,20	1024	131072	1.75	5.00	37
1.60	0.10	24	1024	262144	2.75	5.00	30
1.60	0.10	28	1024	524288	2.75	5.00	30
1.60	0.10	32	1024	1048576	2.75	5.00	30
1.60	0.20	8	2048	8192	1.75	5.00	37
1.60	0.20	10	2840	16384	1.75	5.00	37
1.60	0.20	12	1500	65536	1.75	5.00	37
1.60	0.20	14	2048	1048576	1.75	5.00	40
1.60	0.20	16	2048	4194304	1.75	5.00	40
1.60	0.30	4	3024	8192	0.5	4.00	71
1.60	0.30	6	3024	32768	0.5	4.00	71
1.60	0.30	8	4096	131072	0.5	4.00	71
1.60	0.30	10	2440	1048576	0.5	4.00	71
1.60	0.30	12	1782	8388608	0.5	4.00	71
1.60	0.40	4	4000	8192	0.50	4.00	71
1.60	0.40	6	2048	32768	0.50	4.00	71
1.60	0.40	8	5800	131072	0.50	4.00	71
1.60	0.40	10	3500	524288	0.50	4.00	71
1.60	0.40	12	2100	4194304	0.50	4.00	71

TABLE IV. Parameters of the zero-temperature simulations with $\tilde{J} = J/J_0$, where $J_0 = 1$. H_r is the random field strength, N_{sa} is the number of samples, and N_{eo} is the total number of simulation steps for each system size L.

$\tilde{J}$	H_r	L	N_{sa}	N_{eo}
0.00	1.40, 1.50, 1.55, 1.60, 1.70, 1.80	4	1024	10000000
0.00	1.40, 1.50, 1.55, 1.60, 1.65, 1.70, 1.75, 1.80	6	1024	25000000
0.00	1.40, 1.50, 1.55, 1.60, 1.65, 1.68, 1.70, 1.75	8	1024	35000000
0.00	1.50, 1.55, 1.60, 1.70	10	1024	268435456
0.15	1.50, 1.60, 1.70	4	1024	15000000
0.15	1.50, 1.55, 1.60, 1.65, 1.70	6	1024	25000000
0.15	1.50, 1.55, 1.60, 1.65, 1.70	8	1024	35000000
0.25	1.50, 1.55, 1.60, 1.70	4	1024	25000000
0.25	1.40, 1.50, 1.55, 1.60, 1.65, 1.70	6	1024	25000000
0.25	1.40, 1.50, 1.55, 1.60, 1.65	8	1024	35000000
0.50	1.40, 1.50, 1.55, 1.60, 1.65	4	1024	25000000
0.50	1.40, 1.45, 1.50, 1.55, 1.60	6	1024	35000000
0.50	1.40, 1.45, 1.50, 1.55, 1.60	8	1024	35000000

[1] S. F. Edwards and P. W. Anderson, Theory of spin glasses, J. Phys. F: Met. Phys. **5**, 965 (1975).

[2] Y. Imry and S.-K. Ma, Random-Field Instability of the Ordered State of Continuous Symmetry, Phys. Rev. Lett. **35**, 1399 (1975).

[3] K. Binder and A. P. Young, Spin glasses: Experimental facts, theoretical concepts and open questions, Rev. Mod. Phys. **58**, 801 (1986).

[4] A. P. Young, Ed., *Spin Glasses and Random Fields* (World Scientific, Singapore, 1998).

[5] M. Schechter and P. C. E. Stamp, Correlated random fields in dielectric and spin glasses, Europhys. Lett. **88**, 66002 (2009).

[6] B. E. Vugmeister and M. D. Glinchuk, Dipole glass and ferroelectricity in random-site electric dipole systems, Rev. Mod. Phys. **62**, 993 (1990).

[7] V. Westphal, W. Kleeman, and M. D. Glinchuk, Diffuse Phase Transitions and Random-Field-Induced Domain States of the 'Relaxor' Ferroelectric $PbMg_{1/3}Nb_{2/3}O_3$, Phys. Rev. Lett. **68**, 847 (1992).

[8] D. Sherrington, BZT: A Soft Pseudospin Glass, Phys. Rev. Lett. **111**, 227601 (2013).

[9] M. Schechter and N. Laflorencie, Quantum Spin Glass and the Dipolar Interaction, Phys. Rev. Lett. **97**, 137204 (2006).

[10] S. M. A. Tabei, M. J. P. Gingras, Y.-J. Kao, P. Stasiak, and J.-Y. Fortin, Induced Random Fields in the $LiHo_xY_{1-x}F_4$ Quantum Ising Magnet in a Transverse Magnetic Field, Phys. Rev. Lett. **97**, 237203 (2006).

[11] M. Schechter, $LiHo_xY_{1-x}F_4$ as a random-field Ising ferromagnet, Phys. Rev. B **77**, 020401(R) (2008).

[12] K.-M. Tam and M. J. P. Gingras, Spin-Glass Transition at Nonzero Temperature in a Disordered Dipolar Ising System: The Case of $LiHo_xY_{1-x}F_4$, Phys. Rev. Lett. **103**, 087202 (2009).

[13] J. C. Andresen, C. K. Thomas, H. G. Katzgraber, and M. Schechter, Novel Disordering Mechanism in Ferromagnetic Systems with Competing Interactions, Phys. Rev. Lett. **111**, 177202 (2013).

[14] J. C. Andresen, H. G. Katzgraber, V. Oganesyan, and M. Schechter, Existence of a Thermodynamic Spin-Glass Phase in the Zero-Concentration Limit of Anisotropic Dipolar Systems, Phys. Rev. X **4**, 041016 (2014).

[15] In this work only Ising systems are considered. We note in passing that in dilute Heisenberg dipolar magnets ferromagnetism is unstable also in the absence of an external field [72].

[16] A. A. Middleton, Improved extremal optimization for the ising spin glass, Phys. Rev. E **69**, 055701(R) (2004).

[17] K. Hukushima and K. Nemoto, Exchange Monte Carlo method and application to spin glass simulations, J. Phys. Soc. Jpn. **65**, 1604 (1996).

[18] D. M. Silevitch, D. Bitko, J. Brooke, S. Ghosh, G. Aeppli, and T. F. Rosenbaum, A ferromagnet in a continuously tunable random field, Nature (London) **448**, 567 (2007).

[19] A. P. Young and M. Nauenberg, Quasicritical Behavior and First-Order Transition in the $d = 3$ Random-Field Ising Model, Phys. Rev. Lett. **54**, 2429 (1985).

[20] H. Rieger, Nonequilibrium dynamics and aging in the three-dimensional Ising spin-glass model, J. Phys. A **26**, L615 (1993).

[21] H. Rieger, Critical behavior of the three-dimensional random-field Ising model: Two-exponent scaling and discontinuous transition, Phys. Rev. B **52**, 6659 (1995).

[22] A. T. Ogielski and D. A. Huse, Critical Behavior of the Three-Dimensional Dilute Ising Antiferromagnet in a Field, Phys. Rev. Lett. **56**, 1298 (1986).

[23] J. P. Sethna, K. Dahmen, S. Kartha, J. A. Krumhansl, B. W. Roberts, and J. D. Shore, Hysteresis and Hierarchies: Dynamics of Disorder-Driven First-Order Phase Transformations, Phys. Rev. Lett. **70**, 3347 (1993).

[24] O. Perkovic, K. A. Dahmen, and J. P. Sethna, Avalanches, Barkhausen Noise, and Plain Old Criticality, Phys. Rev. Lett. **75**, 4528 (1995).

[25] G. Bertotti, *The Science of Hysteresis* (Elsevier, Amsterdam, 2006).

[26] D. J. Thouless, J. R. L. de Almeida, and J. M. Kosterlitz, Stability and susceptibility in Parisi's solution of a spin glass model, J. Phys. C **13**, 3271 (1980).

[27] D. S. Fisher and D. A. Huse, Ordered Phase of Short-Range Ising Spin-Glasses, Phys. Rev. Lett. **56**, 1601 (1986).

[28] D. S. Fisher and D. A. Huse, Absence of many states in realistic spin glasses, J. Phys. A **20**, L1005 (1987).

[29] H. G. Katzgraber and A. P. Young, Probing the Almeida-Thouless line away from the mean-field model, Phys. Rev. B **72**, 184416 (2005) (referrred to as KY).

[30] G. Parisi, Infinite Number of Order Parameters for Spin-Glasses, Phys. Rev. Lett. **43**, 1754 (1979).

[31] G. Parisi, Order Parameter for Spin-Glasses, Phys. Rev. Lett. **50**, 1946 (1983).

[32] R. Rammal, G. Toulouse, and M. A. Virasoro, Ultrametricity for physicists, Rev. Mod. Phys. **58**, 765 (1986).

[33] M. Mézard, G. Parisi, and M. A. Virasoro, *Spin Glass Theory and Beyond* (World Scientific, Singapore, 1987).

[34] G. Parisi, Some considerations of finite dimensional spin glasses, J. Phys. A **41**, 324002 (2008).

[35] W. L. McMillan, Domain-wall renormalization-group study of the three-dimensional random Ising model, Phys. Rev. B **30**, 476(R) (1984).

[36] D. S. Fisher and D. A. Huse, Equilibrium behavior of the spin-glass ordered phase, Phys. Rev. B **38**, 386 (1988).

[37] A. P. Young and H. G. Katzgraber, Absence of an Almeida-Thouless line in Three-Dimensional Spin Glasses, Phys. Rev. Lett. **93**, 207203 (2004).

[38] T. Jörg, H. G. Katzgraber, and F. Krzakala, Behavior of Ising Spin Glasses in a Magnetic Field, Phys. Rev. Lett. **100**, 197202 (2008).

[39] H. G. Katzgraber, D. Larson, and A. P. Young, Study of the de Almeida-Thouless Line Using Power-Law Diluted One-Dimensional Ising Spin Glasses, Phys. Rev. Lett. **102**, 177205 (2009).

[40] J. F. Fernández, Evidence against an Almeida-Thouless line in disordered systems of Ising dipoles, Phys. Rev. B **82**, 144436 (2010).

[41] B. Yucesoy, H. G. Katzgraber, and J. Machta, Evidence of Non-Mean-Field-Like Low-Temperature Behavior in the Edwards-Anderson Spin-Glass Model, Phys. Rev. Lett. **109**, 177204 (2012).

[42] A. Billoire, A. Maiorano, E. Marinari, V. Martin-Mayor, and D. Yllanes, The cumulative overlap distribution function in realistic spin glasses, Phys. Rev. B **90**, 094201 (2014).

[43] C. V. Morais, F. M. Zimmer, M. J. Lazo, S. G. Magalhães, and F. D. Nobre, Spin-glass phase transition and behavior of nonlinear

susceptibility in the Sherrington-Kirkpatrick model with random fields, Phys. Rev. B **93**, 224206 (2016).

[44] S. Boettcher and A. G. Percus, Optimization with Extremal Dynamics, Phys. Rev. Lett. **86**, 5211 (2001).

[45] K. Binder, Critical Properties from Monte Carlo Coarse Graining and Renormalization, Phys. Rev. Lett. **47**, 693 (1981).

[46] H. G. Ballesteros, A. Cruz, L. A. Fernandez, V. Martin-Mayor, J. Pech, J. J. Ruiz-Lorenzo, A. Tarancon, P. Tellez, C. L. Ullod, and C. Ungil, Critical behavior of the three-dimensional Ising spin glass, Phys. Rev. B **62**, 14237 (2000).

[47] H. G. Katzgraber, M. Körner, and A. P. Young, Universality in three-dimensional Ising spin glasses: A Monte Carlo study, Phys. Rev. B **73**, 224432 (2006).

[48] D. Sherrington and B. W. Southern, Spin glass versus ferromagnet, J. Phys. F **5**, L49 (1975).

[49] D. Sherrington and S. Kirkpatrick, Solvable Model of a Spin Glass, Phys. Rev. Lett. **35**, 1792 (1975).

[50] B. W. Southern and A. P. Young, Real space rescaling study of spin glass behavior in three dimensions, J. Phys. C **10**, 2179 (1977).

[51] M. Hasenbusch, F. Parisen Toldin, A. Pelissetto, and E. Vicari, Critical behavior of the three-dimensional $\pm J$ Ising model at the paramagnetic-ferromagnetic transition line, Phys. Rev. B **76**, 094402 (2007).

[52] A. K. Hartmann, Scaling of stiffness energy for three-dimensional $\pm J$ Ising spin glasses, Phys. Rev. E **59**, 84 (1999).

[53] A. J. Bray and M. A. Moore, Critical behavior of the three-dimensional Ising spin glass, Phys. Rev. B **31**, 631 (1985).

[54] J. Villain, Equilibrium critical properties of random field systems: New conjectures, J. Phys. France **46**, 1843 (1985).

[55] A. T. Ogielski, Integer Optimization and Zero-Temperature Fixed Point in Ising Random-Field Systems, Phys. Rev. Lett. **57**, 1251 (1986).

[56] B. Ahrens and A. K. Hartmann, Critical behavior of the random-field Ising model at and beyond the upper critical dimension, Phys. Rev. B **83**, 014205 (2011).

[57] B. Ahrens, J. Xiao, A. K. Hartmann, and H. G. Katzgraber, Diluted antiferromagnets in a field seem to be in a different universality class than the random-field Ising model, Phys. Rev. B **88**, 174408 (2013).

[58] N. G. Fytas and V. Martin-Mayor, Universality in the Three-Dimensional Random-Field Ising Model, Phys. Rev. Lett. **110**, 227201 (2013).

[59] P. E. Theodorakis and N. G. Fytas, Random-field Ising model: Insight from zero-temperature simulations, Condens. Matter Phys. **17**(4), 43003 (2014).

[60] A. Aharony, Tricritical points in systems with random fields, Phys. Rev. B **18**, 3318 (1978).

[61] V. Martin-Mayor, Microcanonical Approach to the Simulation of First-Order Phase Transitions, Phys. Rev. Lett. **98**, 137207 (2007).

[62] L. A. Fernández, A. Gordillo-Guerrero, V. Martín-Mayor, and J. J. Ruiz-Lorenzo, First-Order Transition in a Three-Dimensional Disordered System, Phys. Rev. Lett. **100**, 057201 (2008).

[63] L. A. Fernández, A. Gordillo-Guerrero, V. Martin-Mayor, and J. J. Ruiz-Lorenzo, Numerical test of the Cardy-Jacobsen conjecture in the site-diluted Potts model in three dimensions, Phys. Rev. B **86**, 184428 (2012).

[64] D. M. Silevitch, G. Aeppli, and T. F. Rosenbaum, Switchable hardening of a ferromagnet at fixed temperature, Proc. Natl. Acad. Sci. U.S.A. **107**, 2797 (2010).

[65] J. Brooke, D. Bitko, T. F. Rosenbaum, and G. Aepli, Quantum annealing of a disordered magnet, Science **284**, 779 (1999).

[66] M. Schechter and P. C. E. Stamp, Significance of the Hyperfine Interactions in the Phase Diagram of $LiHo_xY_{1-x}F_4$, Phys. Rev. Lett. **95**, 267208 (2005).

[67] M. Schechter and P. C. E. Stamp, The low-T phase diagram of $LiHo_xY_{1-x}F_4$, Phys. Rev. B **78**, 054438 (2008).

[68] A. R. Akbarzadeh, S. Prosandeev, E. J. Walter, A. Al-Barakaty, and L. Bellaiche, Finite-Temperature Properties of $Ba(Zr, Ti))O_3$ Relaxors from First Principles, Phys. Rev. Lett. **108**, 257601 (2012).

[69] D. Sherrington, Relaxor, spin, Stoner and cluster glasses, Phase Trans, **88**, 202 (2015).

[70] M. Manssen and A. K. Hartmann, Aging at the spin-glass/ferromagnetic transition: Monte Carlo simulations using graphics processing units, Phys. Rev. B **91**, 174433 (2015).

[71] S. von Ohr, M. Manssen, and A. K. Hartmann, Aging in the three-dimensional random-field Ising model, Phys. Rev. E **96**, 013315 (2017).

[72] A. Aharony, Absence of ferromagnetic long range order in random isotropic dipolar magnets and in similar systems, Solid State Commun. **28**, 667 (1978).